Clays and Clay Minerals, Vol. 53, No. 4, 389–400, 2005.

CHARACTERIZATION OF EXPANDABLE CLAY MINERALS IN LAKE BAIKAL SEDIMENTS BY THERMAL DEHYDRATION AND CATION EXCHANGE

TOMAS GRYGAR[1,*], PETR BEZDICKA[1], DAVID HRADIL[1], MICHAELA HRUSKOVA[1], KATERINA NOVOTNA[1], JAROSLAV KADLEC[2], PETR PRUNER[2] AND HEDI OBERHANSLI[3]

[1] Institute of Inorganic Chemistry AS CR, Rez, Czech Republic
[2] Paleomagnetic Laboratory, Geological Institute AS CR, Prague, Czech Republic
[3] GeoForschungsZentrum, Potsdam, Germany

Abstract—The sedimentary series from Academician Ridge, Lake Baikal, eastern Siberia, was examined using cation exchange capacity (CEC) to estimate the amount of expandable clay minerals (ECM) and high-temperature X-ray diffraction (HT-XRD) to determine their basic classification. The comparison of the magnetic susceptibility (MS) at sub-millennial resolution and the $\delta^{18}O$ record of a reference Atlantic core (ODP 980) was used to create an age model. The most closely studied part of the series covered the major part of the last glacial cycle (120–20 ky BP). The HT-XRD analysis is based on monitoring the course of ECM dehydration with 5ºC steps between 25 and 250ºC and enabled us to improve the discrimination between ECM, chlorite and micas. The CEC obtained at millennial resolution showed that the neoformation of ECM in warmer periods of the last interglacial was either insignificant or fully compensated by their dissolution or dilution. The CEC record was correlated with the main climatic stages in the period studied. Both MS and CEC records reflected the environmental changes at about millennial resolution, including climatic instabilities between 117 and 73 ky BP (late MIS5).

Key Words—Cation Exchange Capacity, Lake Baikal, Lake Sediments, Paleoclimate, Russia, Thermal Dehydration, XRD.

INTRODUCTION

Lake Baikal is one of the most valuable terrestrial climatic archives covering the Upper Pliocene, the entire Pleistocene and the Holocene (*e.g.* Grachev *et al.*, 1998; Müller *et al.*, 2001; Kravchinsky *et al.*, 2003); according to Antipin *et al.* (2001) it extends to the Miocene. The diagnostic value as well as the limitations of clay minerals as paleoenvironmental indicators seem well established (Singer, 1979/1980; Thiry, 2000). Traditional measures like smectite or kaolinite percentage work well in environments with temporarily very intense chemical weathering or they may be used to trace the variations in the sediment source area. However, Lake Baikal is situated in eastern Siberia, where very cold periods with practically no chemical weathering (glacials or stadials) alternated with periods of moderate climate (interglacials and interstadials). Additionally, the changes in the Quaternary climate, corresponding to the periodicity of the insolation curve in high latitudes of the northern hemisphere (climatic optima usually lasting up to ~10 ky), are rather short with respect to the sluggishness of the formation of clay minerals. Although those facts are rather unfavorable for paleoclimatic interpretation based on clay minerals (Thiry, 2000), such attempts have been made (Yuretich *et al.*, 1999; Solotchina *et al.*, 2002; Horiuchi *et al.*, 2000; Fagel *et al.*, 2003). However, the clay mineralogy in sediments may be a function of the transport mechanism or the sediment source area, *i.e.* an environmental function.

The most reliable ways to characterize expandable clay structures in polymineralic materials are based on the variability of their basal spacings using diffraction methods. Currently, the most common way is to compare XRD patterns of completely solvated (hydrated, glycol or glycerol solvated) and completely de-solvated specimens by a set of two or several *ex situ* XRD measurements. Since the 1980s, more detailed insight into dehydration has become possible through use of *in situ* high-temperature diffraction measurements that can visualize the course of dehydration by almost continuously recording diffraction patterns. The first HT-diffraction experiments, using X-rays and proportional or scintillation detectors, were very time consuming as the data acquisition at each hydration stage lasted for up to several hours (Moore and Hower, 1986; Collins *et al.*, 1992). The developments of diffraction instrumentation, especially the availability of faster, position-sensitive detectors (Graf von Reichenbach and Beyer, 1994; Bérend *et al.*, 1995; Cases *et al.*, 1997), made it possible to monitor the process with much better resolution. The HT-XRD and neutron diffraction are mainly used in kinetic and structural studies of pure, single-component clay minerals, but not for the analysis of polymineralic specimens.

The dehydration of expandable clay minerals is not a simple reaction. The principle hydration stages are denoted as 2 layer (14–16 Å), 1 layer (12–13 Å), and

* E-mail address of corresponding author:
grygar@iic.cas.cz
DOI: 10.1346/CCMN.2005.0530407

0 layer (~10 Å) hydrates (Bérend *et al.*, 1995; Cases *et al.*, 1997). Vermiculite (Weiss *et al.*, 1994; Graf von Reichenbach and Beyer, 1994; Ruiz-Conde *et al.*, 1996; Marcos *et al.*, 2003) and montmorillonite (Moore and Hower, 1986; Collins *et al.*, 1992; Ruiz-Conde *et al.*, 1996) are de- and re-hydrated *via* several, sometimes coexisting, relatively well defined intermediate states including interstratified 2/1 and 1/0 hydrates. The dehydration is controlled by the partial pressure of water, *i.e.* it proceeds very similarly both on heating and on evacuation (Marcos *et al.*, 2003). The reaction kinetics (Laureiro *et al.*, 1996; Bray *et al.*, 1998) also play an important role, and some influence of the particle size can be expected. The course of the dehydration would therefore be controlled by the composition and pressure of the surrounding atmosphere, the variety of expandable clay mineral, the interlayer cations, and the reactant particle size. This situation resembles that in thermal analysis, where the maximum number of variables must be kept constant during all experiments and the samples analyzed must be compared with reference compounds.

In this work, we tested HT-XRD for the analysis of a complex assemblage of the bottom sediments from Lake Baikal. The aim was to establish the paleoenvironmental conditions from the clay minerals and to develop a tool complementary to the biogenic indicators, of which the most common is a diatom record (Grachev *et al.*, 1998; Edlund and Stoermer, 2000; Prokopenko *et al.*, 2001a). Total cation exchange capacity (CEC) seems to be the most reliable means of estimating the amount of expandable clay structures in mineral mixtures (Kaufhold *et al.*, 2002). We chose a very convenient method using Cu-trien, as described by Meier and Kahr (1999). The sediment studied was obtained from coring site VER98-1-13 in the Academician Ridge (Figure 1), *i.e.* from the same place as several previous studies (Peck *et al.*, 1994; Grachev *et al.*, 1998; Horiuchi *et al.*, 2000; Prokopenko *et al.*, 2001a; Müller *et al.*, 2001; Fagel *et al.*, 2003; Kravchinsky *et al.*, 2003; Demory *et al.*, 2005). The age of the core studied in this work was obtained by correlating its magnetic susceptibility record with the isotopic composition of foraminifera from a reference Atlantic core for which dates were available (ODP 980, McManus *et al.*, 1999, 2002) using an approach suggested by Peck *et al.* (1994) and Kravchinsky *et al.* (2003). The aims of this work were to test two novel approaches to the analysis of late

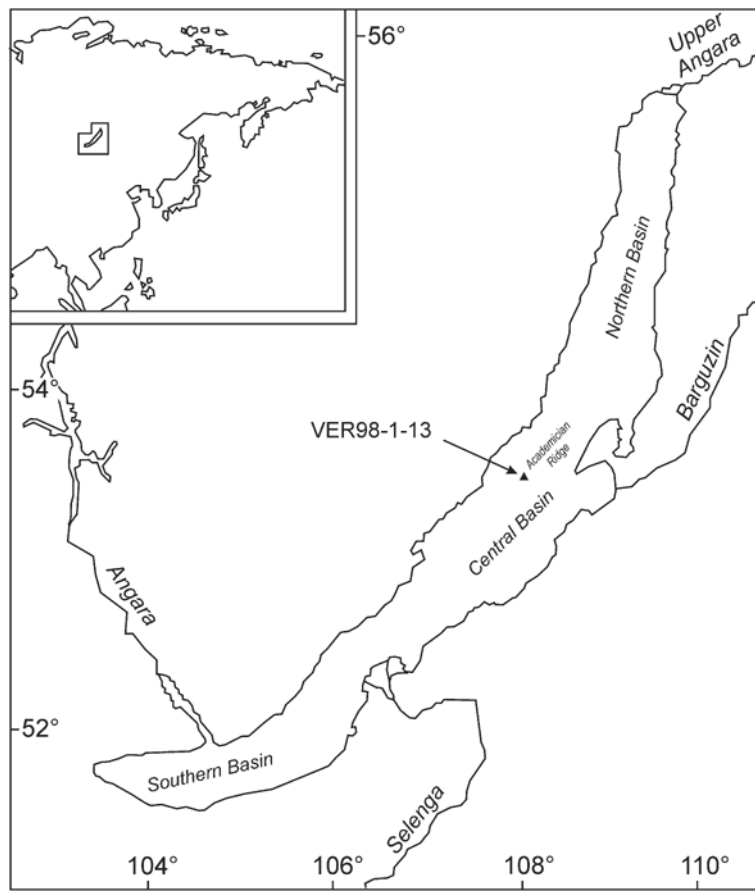

Figure 1. Position of the coring site VER98-1-13 (triangle) in Lake Baikal.

https://doi.org/10.1346/CCMN.2005.0530407 Published online by Cambridge University Press

Quaternary lacustrine sediments and to assess the paleoclimatic significance of the clay mineral characteristics obtained therefrom.

MATERIALS AND METHODS

VER98-1-13 core, magnetic measurement, age model

Samples were obtained from the pilot (gravity) and the piston (hydraulic) cores of VER98-1-13 with the total (composite) length of ~12 m, retrieved from the western part of the Academician Ridge, Lake Baikal, at latitude 53.561ºN and longitude 108.011ºE, at a water depth of 335 m (Figure 1). The cores had been stored in sealed Al tubes at 4ºC in GFZ Potsdam, Germany, since 1998. In 2003 the tubes were opened and the inner parts of the cores were sampled using polystyrene boxes, with an inner volume of 7 cm^3, to measure their magnetic susceptibility (MS). The lithology was similar to that reported previously for other sedimentary cores from Academician Ridge (Peck *et al*., 1994; Müller *et al*., 2001; Fagel *et al*., 2003): diatomaceous mud alternated with clayey layers with colors ranging from bluish or greenish gray to brown.

The MS was measured with a vertical spacing of 2.2 cm. Low-field volume MS was measured with a Kappabridge KLY-3S (sensitivity of 1.2×10^{-8} SI). The age was obtained using the procedure suggested by Peck *et al*. (1994) by comparing the MS log with the $\delta^{18}O$ of foraminifera (SPECMAP). In our work, we used a reference isotopic record from Atlantic core ODP980 (McManus *et al*., 1999, 2002).

Analytical techniques, reference phases

High-temperature powder XRD was performed in an Anton Paar HTK16 high-temperature chamber with PANalytical X'Pert PRO diffractometer (CoKα radiation, X'Celerator multichannel detector). The naturally wet samples (~50% weight loss on drying at 50ºC) were taken from the boxes for the MS measurement, suspended in methanol and deposited in a layer <0.1 mm thick on the Pt heated element. Methanol was much more convenient for the thin-layer preparation than water; the thermal behavior of the samples was the same with both solvents. The diffraction patterns were scanned from 4 to 40º2θ with steps of 0.016º/60 s (*i.e.* ~20 min per scan) over a temperature range of 25 to 250ºC with steps of 5ºC, *i.e.* each data set contained 44 patterns. The total duration of the HT-XRD experiment was 18 h. The results were compared with those obtained from the reference saponite SapCa-2, nontronite NAu-2, montmorillonites SAz-1, STx-1 and SWy-2, and interstratified illite-smectites ISMt-2 and ISCz-1, obtained from the Source Clays Repository of The Clay Minerals Society, West Lafayette, Indiana, USA. Homoionic Mg-forms were prepared by triple shaking for 24 h with an excess 1 M solution of $MgCl_2 \cdot 6H_2O$ with centrifugation (14 min/9800 rpm) after each step followed by five 24 h washings with water. The final supernatant liquid was free of chlorides according to the $AgNO_3$ test. Reference Mg-rich vermiculite was a specimen collected from a weathered ultrabasic zone at Letovice, Czech Republic (Weiss *et al*.,, 1994). The integral intensities of selected diffraction lines were obtained by the peak fitting module in *OriginPro* 7.0 (OriginLab, Northampton, MA, USA) using either pseudo-Voigt peaks (sediments) or plain integration above a linear baseline (reference minerals).

Conventional oriented specimens were prepared by slow sedimentation of suspension of selected samples on a glass slide. Suspensions were dried in air and then solvated by ethylene glycol vapors at 70ºC. Basal spacing of expandable clay structures in air-dried and glycol-solvated samples was measured by conventional XRD (CuKα radiation, diffracted beam monochromator, scintillation detector, Siemens D5005, Bruker). Then these oriented samples were solvated by liquid glycerol and measured again.

Total CEC was determined by a Cu-trien method (Meier and Kahr, 1999). An aqueous solution of Cu-trien (1,4,7,10-tetraazadecane copper sulfate, $[Cu(C_6N_4H_{18})]SO_4$, 9 mM) was prepared by mixing 1000 mL of a solution of 1.596 g of anhydrous $CuSO_4$ (for analysis, Lachema, Czech Republic) and 100 mL of a solution of 1.463 g of ligand (purum, >97%, Fluka) in distilled water. Samples (0.3 g) dried at laboratory conditions and ground in an agate mortar were transferred to 50 mL flasks, re-wetted with few mL of distilled water, and mixed with 7.5 mL of Cu-trien solution. The suspension was diluted to 50 mL by distilled water. After 5 min, the suspension was centrifuged at 9800 rpm for 7 min. The supernatant liquid was filtered off, and the residual concentrations of Cu and concentrations of Mg and Ca in solution were determined using atomic absorption (Cu, Mg) or emission (Ca) spectroscopy with AAS-3 (Carl Zeiss, Jena, Germany).

RESULTS

MS log and age model

The age model for the core studied is shown in Figure 2; the magnetic susceptibility record of the Baikal core was compared to the isotopic composition of sea water obtained from a reference core of the Atlantic Ocean sediment taken from McManus *et al*. (1999, 2002). The principle of this procedure for indirect dating of sediments from the Academician Ridge was introduced by Peck *et al*. (1994) and confirmed by Kravchinsky *et al*. (2003). The accuracy of the age model is comparable to the resolution of the actual North Atlantic reference core, *i.e.* 1–5 ky (mean distance of neighboring points 1.2 ky), and could contain some uncertainty related to non-synchronous timing of the climatic changes in Atlantic Ocean and Eastern Siberia.

https://doi.org/10.1346/CCMN.2005.0530407 Published online by Cambridge University Press

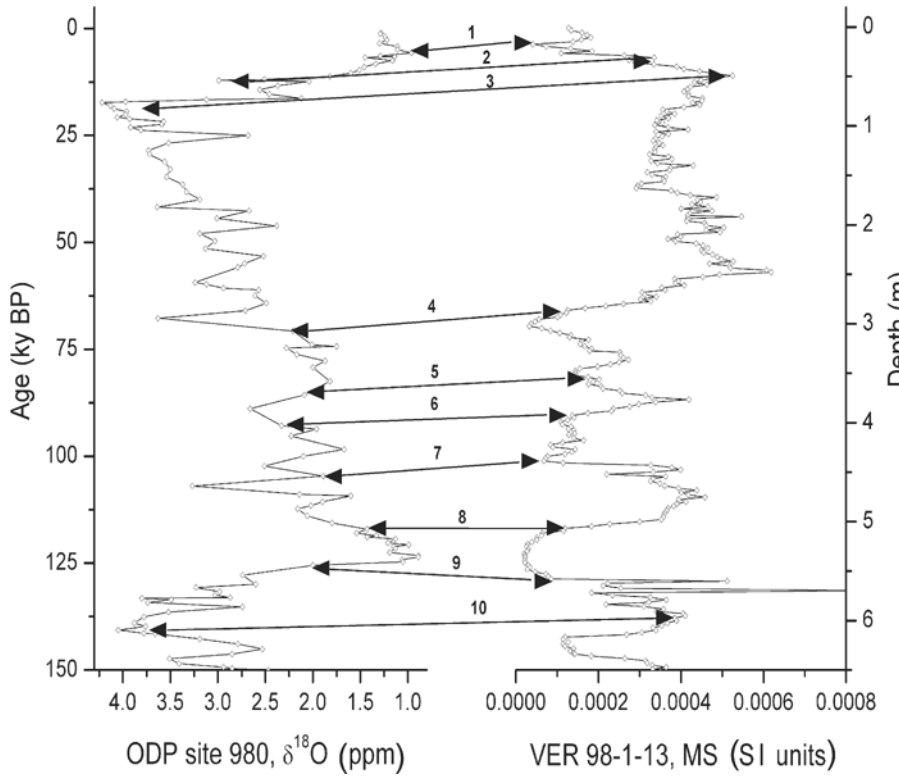

Figure 2. The reference record of $\delta^{18}O$ of sea water (McManus *et al.*, 1999, 2002, left curve) and MS log of the Lake Baikal core VER98-1-13 (right curve). The tie points for the age model are indicated by triangles connected by lines and are listed in Table 1.

Ten tie points were used of which three corresponded to cold extremes, namely point 2, the Younger Dryas, point 3, the last cold minimum, and point 10, a cold minimum in late MIS6; the rest of the points were assigned to boundaries between warm and cold periods. The dating of the other samples was obtained by linear interpolation between the tie points.

There are at least two reasons for a straightforward relationship between the MS pattern and actual paleoclimate: dilution of magnetic components by the diamagnetic diatom frustules (Peck *et al.*, 1994; Kravchinsky *et al.*, 2003), and/or reductive dissolution of magnetite (Demory *et al.*, 2005); both processes are typical for warm periods. The mean estimated sedimentation rate in the top 6 m is 4.5 cm/ky, quite similar to the mean rate of 5.12 cm/ky found by Peck *et al.* (1994) for Academician Ridge cores covering the last 200 ky. This sedimentation rate is surprisingly stable over a long period. Rates of 2.6–5.8 cm/ky were found for Academician Ridge in the Pliocene/Pleistocene transition (3.4–2.2 My BP) with a much warmer climate than today (Müller *et al.*, 2001), and an almost constant sedimentation rate of 3.9 cm/ky for the last 6.7 My was reported by Kravchinsky *et al.* (2003).

Table 1. Tie points used for the age model according to Figure 2. Reference sedimentary series ODP980 was taken from McManus *et al.* (1999, 2002).

Tie point	Sediment depth (m)	Description of tie point	Age (ky)
1	0.174	Warm maximum	6
2	0.310	Younger Dryas	12
3	0.493	Cold minimum of the last glaciation	17
4	2.955	Transition MIS5a/MIS4	71
5	3.654	Warming MIS5b/MIS5a	86
6	3.927	Cooling MIS5c/MIS5b	93
7	4.407	Onset of stable part of MIS5c	105
8	5.068	Cooling MIS5e/MIS5d	116
9	5.578	Warming MIS6/MIS5e	125
10	5.952	Cold minimum of late MIS6	141

https://doi.org/10.1346/CCMN.2005.0530407 Published online by Cambridge University Press

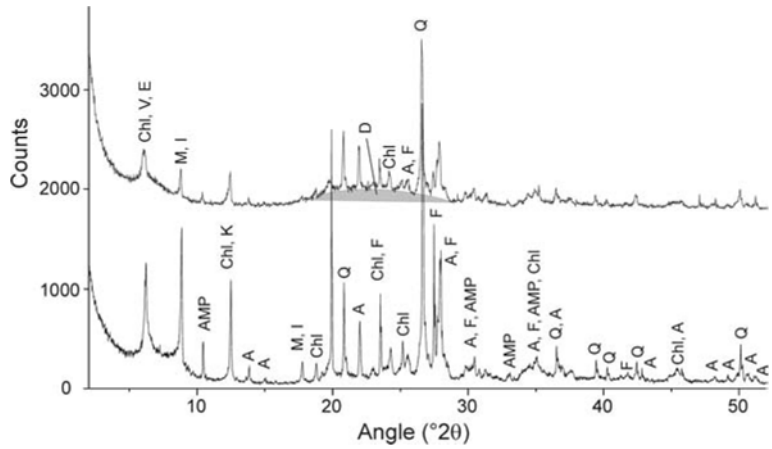

Figure 3. A typical powder XRD pattern of a dry sediment sample. Phase abbreviations: E: expandable clay minerals, V: vermiculite, Chl: chlorite, M+I: macroscopic mica and illite, AMP: amphibole, A: Na,Ca-feldspar, F: K-feldspar, K: kaolinite, Q: quartz, D and gray area: biogenic silica (diatom frustules). Upper curve: sample from the warmest stage in the range studied (120 ky BP, the Eemian MIS5e), lower curve: sample for the coldest stage studied (19 ky BP, the last glacial maximum MIS2).

Basic mineralogy of the sediments

The mineralogical composition obtained by conventional powder XRD (Figure 3) is very similar to that reported by Horiuchi *et al*. (2000), Müller *et al*. (2001), Solotchina *et al*. (2002) and Fagel *et al*. (2003) for fine-grained sediments from the Academician Ridge. General minerals like quartz, muscovite, feldspars and kaolinite, and minerals with varying contents such as amphibole, illite, chlorite and an assemblage of expandable clay minerals are present. An attempt to analyze the mixture of clay minerals using ethylene glycol solvation was only partially successful because the reflections of glycol-solvated oriented specimens were rather wide (FWHM>1°2θ) with a flat diffraction maximum near 17.0 Å. Reliable discrimination between clay minerals is difficult if smectite and fully expandable vermiculite coexist with smectite-rich mixed-layered structures, as is probably the case in the sediments studied (Solotchina *et al*., 2002; Fagel *et al*., 2003). The positions of diffraction lines of expanding structures in samples solvated with glycerol were scarcely visible above the baseline, and although some expansion was recognized, it was impossible to distinguish between smectite and vermiculite.

HT-XRD of clay minerals

An example of thermal evolution of the sediment XRD pattern is shown in Figure 4 for which the XRD patterns were smoothed with a 5 point Fourier filter to suppress the noise. The range used for the data processing of scans was 8.8–16.3 Å (6.3–11.7°2θ with CoKα). The first scan was acquired at 25°C, immediately after evaporation of the excess liquid from the suspension. In this first scan, a very intense and rather broad basal reflection of the assemblage of expandable clay minerals (E) completely overlapped the chlorite 001 reflection. The chlorite basal reflection became visible above ~50°C, when a triplet (E1, E2, E3) of basal reflections was developed from the original reflection E with the components shifting continuously to higher angles. Their position further shifted towards the mica 001 reflection at ~10 Å, overlapped it above 150°C, and at 250°C the ECM, M and I reflections merged to a strongly asymmetrical joint line with summary FWHM of ~0.3°. The thermal dependence of the position of 001

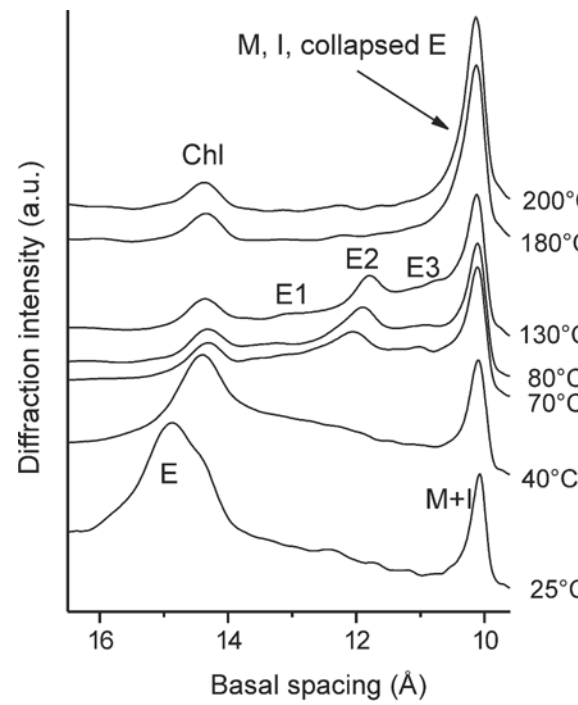

Figure 4. Typical HT-XRD patterns of thin layers of sediment sample from warm MIS5a. The assemblage of expandable clays, E, and chlorite, Chl, is separated into the components including expandable clay classes E1, E2 and E3 on heating. Other phase abbreviations are as in Figure 3. The patterns were smoothed by a 5 pt Fourier filter, plotted with manual shifts along the y axis. The actual temperature is denoted for each XRD pattern.

https://doi.org/10.1346/CCMN.2005.0530407 Published online by Cambridge University Press

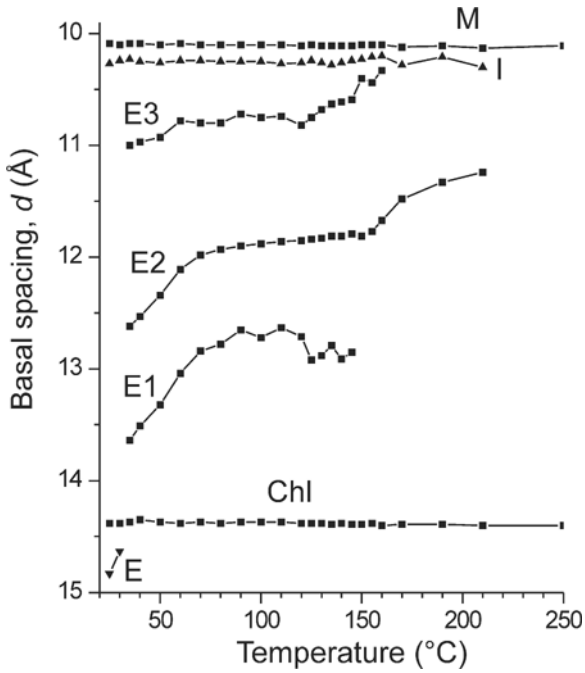

Figure 5. The change of the position of basal spacing of expandable clay minerals in the sample from warm MIS5a (as in Figure 4). The diffraction line position as well as illite and macroscopic mica separation was performed by deconvolution to pseudo-Voigt components. The phase notation is the same as in Figure 3.

reflections of the clay structures is shown in Figure 5, the list of their parameters at 100ºC is summarized in Table 2, and their fractional integral intensities at 100ºC are listed in Table 3. A very similar thermal dependence was observed in all samples analyzed, as is obvious from a small scatter of the reflection parameters for different samples (Table 2). Illite (clay mica) and macroscopic mica (muscovite or biotite) were distinguished by the deconvolution of their overlapping, obviously asymmetrical diffraction line at ~10 Å, of which full profile fitting was impossible with a single pseudo-Voigt component. The processing of the entire series yielded a very consistent pair of their positions and widths with only relative ratio variations (Tables 2 and 3).

In scans at the final temperature of 250ºC, a reflection was recognized at 12.3 Å with an area <1% of the area of the diffraction at ~10 Å of all mica-like structures. This line with roughly the same area was found in all samples subjected to HT-XRD. Because the

Table 2. List of mean positions (d) and widths (FWHM) of 001 diffraction lines of clay minerals in sediments and reference ECM in HT-XRD scans at 100ºC. The standard deviations are given in parentheses at sediment samples (N = 18).

Species in sediments[1]	d (Å)	FWHM (º2θ)
Chl	14.39 (0.03)	0.25 (0.04)
E1	12.79 (0.18)	1.2 (0.2)
E2	11.92 (0.03)	0.43 (0.10)
E3	10.82 (0.10)	1.2 (0.1)
I	10.25 (0.02)	0.38 (0.05)
M	10.10 (0.01)	0.17 (0.01)
Reference phases[2]	**d (Å)**	**FWHM (º2θ)**
SAz-1	12.6	1.4
Mg-SAz-1 (Mg)	12.5	1.6
Vermiculite, flakes	12.3	0.46
Mg-STx-1 (Mg)	12.3	1.1
Mg,Ca-STx (Ca,Mg)	12.0	1.1
STx-1 (Ca>Mg>Na)	11.5	1.1
ISMt-2, I-S 60/40	10.8	0.8
ISCz-1, I-S 70/30	10.6	0.9

[1]Phase abbreviations as in Figure 3.
[2]The composition of the interlayer (exchangeable) cations is given in parentheses.

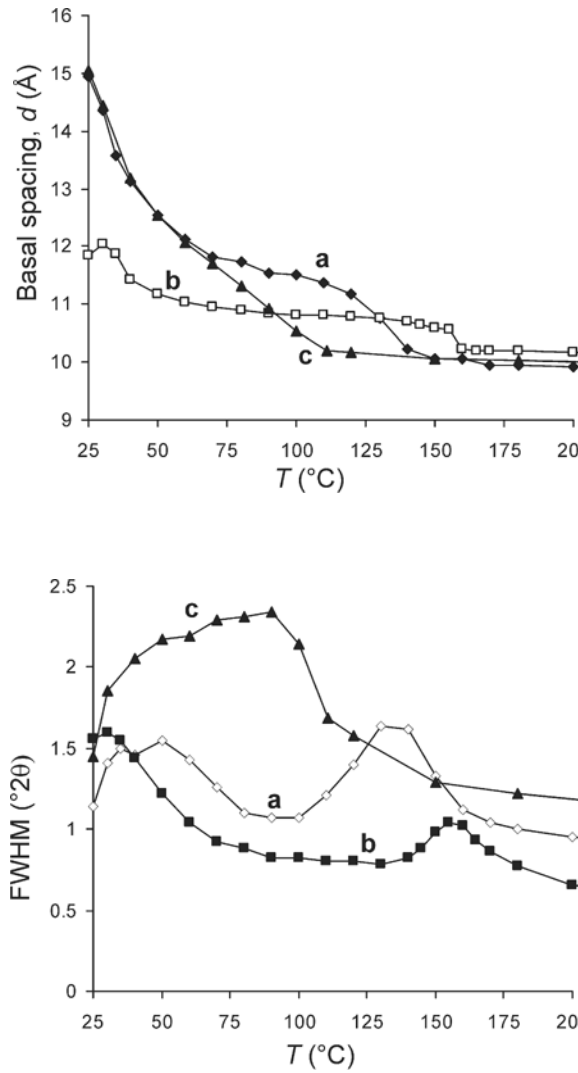

Figure 6. Variation of the main basal spacing d_{001} of reference clay minerals (uppermost) and line width FWHM (lowermost) of three expandable clay minerals during HT-XRD. Curve labels: (a) montmorillonite STx-1, (b) interstratified illite-smectite 70/30 ISMt-2, (c) nontronite NAu-2.

https://doi.org/10.1346/CCMN.2005.0530407 Published online by Cambridge University Press

Table 3. Integral intensities of clay minerals in HT-XRD scans at 100ºC normalized to total diffraction area between 6.3 and 11.7º2θ, climatic conditions and cation exchange capacities.

Depth (m)	Age (ky)	Climatic stage (conditions[1])	Percentage of areas of basal diffraction lines[2] Chl	E1	E2	E3	I	M	CEC[3]
0.127	<2	MIS1 (IG)	7	18	14	23	27	11	8.8
0.583	19	MIS2 (G)	6	19	20	25	19	11	8.9
0.850	24	MIS2 (G)	4	18	16	36	16	10	11.3
1.036	27	MIS3/MIS2 (G)	4	17	22	29	15	12	10.4
1.195	31	MIS3 (cooling)	3	19	19	30	17	11	10.5
1.309	33	MIS3 (cooling)	3	22	15	34	11	15	9.8
1.746	44	MIS3 (S)	4	16	19	28	16	17	10.1
2.120	52	MIS3 (S)	2	13	21	39	15	10	11.4
2.504	61	MIS4 (S)	6	12	11	24	35	12	11.4
2.820	66	MIS4 (S)	9	14	11	26	27	13	10.4
3.250	80	MIS5a (IG)	20	10	10	25	24	10	7.6
3.502	85	MIS5b (cold)	11	32	9	24	8	16	5.5
3.563	86	MIS5b (cold)	12	23	8	21	26	10	9.8
4.040	100	MIS5c (IG)	10	13	22	21	23	11	7.7
4.339	106	MIS5d/MIS5c (warming)	8	21	5	35	21	10	8.4
4.521	112	MIS5d (cold)	12	10	11	31	23	13	6.5
4.614	115	MIS5d (cold)	9	22	7	29	17	16	9.4
5.208	120	MIS5e (IG)	10	24	24	22	13	7	7.6

[1]G glacial (very cold), S stadial (cold), IG interglacial (warm).
[2]Phase abbreviations as in Figure 3, their diffraction line characteristics according to Table 2.
[3]mmol M^{2+}/100 g

identical reflection was also found in the initial 25ºC scans (originally it was overlooked, because it is located on the slope of dominant diffraction E), it could be assigned to interstratified mica-chlorite; this phase was also found by Fagel *et al*. (2003) in two neighboring coring sites. In intermediate temperatures, that species was overlapped by much more abundant, partly dehydrated, expandable structures E1 to E3. The mica-chlorite content was so small that its presence was not evaluated.

The species E1, E2 and E3 were identified by comparing their HT-XRD behavior with that of the reference clay minerals with similar interlayer cations under the same experimental conditions (Figure 6, Table 2). In accordance with previous studies (Collins *et al*., 1992; Bérend *et al*., 1995; Bray *et al*., 1998), there is a unique basal reflection shifting towards higher angles on dehydration for finely crystalline clay minerals. The only exception to the rule 'one mineral-one basal diffraction line' is probably a macroscopic vermiculite that could produce split reflections during very slow, near-equilibrium dehydration (Graf von Reichenbach and Beyer, 1994; Weiss *et al*., 1994; Marcos *et al*., 2003); this splitting was not observed under our rather fast dehydration. The three reflections, E1–E3, therefore correspond to at least three individual expandable clay minerals, with E2 being the most crystalline, and E1 and E3 with the XRD coherence length comparable to the reference smectites and illite-smectite specimens.

The principle of the visualization of expandable clay minerals by HT-XRD is demonstrated in Figure 6. It is based on the change of the diffraction line widths (FWHM) during dehydration and varying thermal stability of the individual minerals and their hydrated interlayer cations. Bray *et al*. (1998) showed that FWHM of smectite subjected to dehydration is largest when more hydration states coexist in the specimen. In some cases, *e.g*. interstratified illite-smectite samples ISMt-2 (Figure 6) and ISCz-1 (not shown), the initial hydration state is most disordered. This could cause substantial worsening of the detection limit of the interstratified clay minerals in the polymineralic mixture of the sediments. The FWHM of the two reference interstratified illite-smectites continuously decreases and reaches its minimum at ~100ºC, when 1-layer hydrate of the expandable layers is formed. A similar effect of peak sharpening is probably responsible for the visualization of E3 in sediments at >50ºC but not in the initial scans. The optimized separation of the basal diffraction lines at a certain temperature range is demonstrated by the model example of nontronite and montmorillonite (Figure 6): at 100–120ºC the phases would be best resolved if they were present in a physical mixture. The clay mineral assemblage of the Lake Baikal sediments was actually best resolved at that same temperature range.

To reveal a possible difference between individual specimens of smectites with the same cation in the interlayer space, we studied homoionic Mg-exchanged minerals (Figure 7). The basal spacing of the dehydration intermediates was assigned according to Cases *et al*. (1997) as a 2-layer hydrate producing the plateau at ~14.5 Å (two substages were distinguished) and 1-layer

https://doi.org/10.1346/CCMN.2005.0530407 Published online by Cambridge University Press

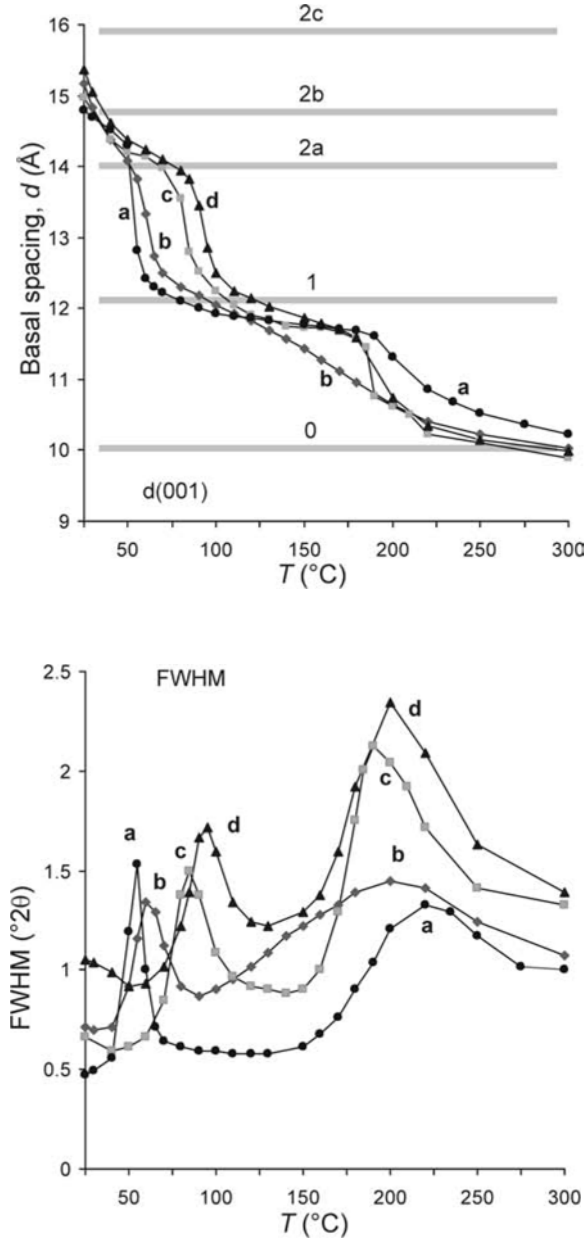

Figure 7. Variation of the main basal spacing d_{001} of reference clay minerals (uppermost) and line width FWHM (lowermost) of homoionic Mg-smectites during HT-XRD. The basal spacing of hydrate states 0 and 1 and substrates 2a, 2b and 2c were taken from Cases *et al.* (1997) and are indicated by rectangles and the number of water layers in the top figure. Curve labels: (a) saponite SapCa-2, (b) montmorillonite SWy-2, (c) montmorillonite STx-1, (d) smectite 'Cheto' SAz-1.

hydrate producing the plateau at ~12.0 Å. The basal spacing of the plateaux depended slightly on the kind or type of the ECM studied, but the stability regions of their individual hydrates varied within several tens of ºC. According to Cases *et al.* (1997) and Collins *et al.* (1992), 1-layer hydrates of Mg-vermiculite and Mg-montmorillonite are more resistant to further dehydration than corresponding Ca-forms. This is probably the reason for the basal spacing in the 100ºC scan to increase in the order STx-1 < Mg,Ca-STx-1 < Mg-STx-1 (Table 2). However, in spite of these differences between individual smectites, the 100ºC scan can reliably distinguish smectite or vermiculite on one hand and illite-smectite (or possibly illite-vermiculite) on the other hand.

The basal spacing and thermal stability of E2 correspond best to Mg,Ca-smectite or vermiculite. The species E2 is obviously the most structurally uniform among the expandable clay minerals present in the Lake Baikal sediments: between 70 and 140ºC, its FWHM is ~0.4º2θ scale and is very similar to that of the chlorite component of the sediment and to the macroscopic reference vermiculite (Table 2). E1 and E3 have worse crystallinity, their FWHM is between 1.0 and 1.2º2θ, *i.e.* very close to that of all the reference ECM studied (0.6–1.5º at ~100ºC, Table 2). According to the position and FWHM of its basal diffraction, E3 is closest to the interstratified illite-smectite ISMt-2. The basal spacing of E1 at ~100ºC is much larger than that of any reference clay minerals studied and hence E1 cannot be identified using the current set of reference minerals.

Total CEC and Mg/Ca in exchangeable cations

The supernatant liquid, after treating the samples with Cu-trien solution, was analyzed by atomic absorption spectroscopy (AAS) and atomic emission spectroscopy (AES) to determine total dissolved cations. The Cu residual concentration thus ascertained was used to estimate CEC in mmol of M^{2+}/100 g of dry samples. Major exchangeable cations are Ca^{2+} and Mg^{2+}; the Li^{+}, Na^{+}, K^{+} and Sr^{2+} contents were less than the determination limit of AES (*i.e.* <2 wt.% of Mg+Ca). The mean relative difference between the Cu consumed (ΔCu^{2+}, mmol/100 g of dry sample) and the sum of Ca^{2+} and Mg^{2+} (mmol/100 g of dry sample), $(\Delta Cu^{2+} - Ca^{2+} - Mg^{2+})/\Delta Cu^{2+}$, was −7%, *i.e.* the average Cu consumption was slightly (statistically insignificantly) less than the sum of Ca+Mg evolved to solution. This indicates that Cu^{2+} adsorption and complex hydrolysis did not play a significant role. That systematic error was, however, less than the variance of ΔCu^{2+} within the profile (total range of ΔCu^{2+} was 4.4 to 12.9 mmol M^{2+}/100 g, mean CEC = 9.3, σ =1.22, σ_{REL} = 13%, N = 151).

The mean Mg/Ca molar ratio in the profile was 0.23 (σ = 0.04, N = 151). As follows from the basal spacing of E2 at 100ºC (Table 2), a substantial fraction of the total exchangeable Mg should actually be present in E2.

Correlations

The most significant correlation between the percentages of the individual minerals listed in Table 3 is the statistically significant indirect proportionality between relative concentrations of chlorite and the sum of E2+E3:

https://doi.org/10.1346/CCMN.2005.0530407 Published online by Cambridge University Press

Table 4. Clay mineralogical (CM) zones and their correlation with global climatic stages (MIS). Ranges of CEC, relative contents of clay minerals (estimated from the ratio of their integral intensities of 001 reflections (data from Table 3)), and main climatic stages.

CM zone	Age (ky)	CEC (mmol/100 g)	Relative contents[1] (XRD) (%) Chl	E2	E3	Corresponding MIS, general conditions
I	13–22	7.9–10.2	6	20	25	MIS2, extremely cold and dry
II	23–55	9.1–12.3	3	19	33	MIS3, cold, dry, unstable
III	55–70	9.8–11.9	5	16	30	MIS4, cold
IV	75–85	5.3–9.8	16	10	25	MIS5a, warm
V	85–95	5.4–11.1	11	9	23	MIS5b, colder
VI	98–113	6.5–9.5	10	13	29	MIS5c, warm
VII	115–117	8.6–9.6	9	7	29	MIS5d, cold
VIII	120–126	4.7–7.6	10	24	22	MIS5e, warm, humid

[1]Phase abbreviations as in Figure 3

$$(E2+E3) = 52 - 1.2 \times Chl,\ r = 0.692,\ N = 18$$

Also, CEC is indirectly proportional to the relative area of the chlorite diffraction:

$$CEC = 11.1 - 0.25 \times Chl,\ r = 0.655,\ N = 18$$

On the other hand, the relative areas of CEC and (E2+E3) are directly proportional, though the regression coefficient is not statistically significant. Both of these relationships show that the CEC and HT-XRD results are interrelated. The qualitative general evaluation of the variations of CEC and relative ratio of the basal diffractions of clay minerals is summarized in Table 4.

DISCUSSION

Characterization of clay minerals in sediments

The E2 species was assigned as Ca,Mg-smectite or vermiculite and E3 as interstratified illite-smectite. There is a lack of reference compounds approaching the behavior of E1 species: its basal spacing at 100ºC (12.5–13.2 Å) is larger than that of any 1-layer hydrate of Ca- or Mg-smectite or vermiculite reported in the literature or available in this study. Because of the general presence of chlorite in all sediments, E1 could be partly weathered chlorite (interstratified chlorite-expandable phase), or some initial stage of the chlorite hydration (weathering). This hypothesis is supported by the observation that CEC correlates with E2+E3.

Verification of age model

The CEC record can easily be correlated with the main climatic stages in the period 117–23 ky BP (Table 4, Figure 8). The discrepancies in the timing of the changes in CEC and MS and conventional boundaries of MIS could be partly attributed to the uncertainty of our age model, but they are probably caused by a different impact of the individual climatic changes in the Atlantic region on the environmental changes in the Eastern Siberia. For example, the changes in MS and CEC records between CM zones IV and III at 75–65 ky BP and their relation to the MIS5a/MIS4 transition are not simply synchronous. The CEC increased extremely sharply at 75–73 ky BP, in agreement with the erosion event at ~75 ky BP and a decrease in the diatom frustules content found by Prokopenko *et al.* (2001b). Those authors attributed that change to the Heinrich event H7, that preceded the conventional MIS5a/MIS4 transition by ~5 ky. The CEC change hence coincides with a well defined environmental change in the Baikal watershed than does SPECMAP. Another verification of the relevance of the CEC record is that even small variations in the MS record in the CM zone VI (MIS5d,c) are clearly visible in the CEC record and can be correlated to the climatic events: There is a distinct but small-amplitude variation in MS in 106–101 ky BP and a much more pronounced maximum of CEC at 106–103 ky BP. At 103–100 ky BP, Prokopenko *et al.* (2001a) found a sharp, short-term decrease in the diatom frustules content explained as a dramatic cooling event. This good agreement substantiates the paleoenvironmental significance of MS and CEC records, and also verifies our age model. To understand the CEC variation, it is necessary to develop a corresponding model, because the CEC pattern obtained disagrees with some previous reports and assumptions based, as they were, on the results of substantially different experimental techniques.

Environmental interpretation

The longest period with the highest CEC values in sediments lasted from 73 to 23 ky BP, *i.e.* it started by the end of the last interglacial warm period MIS5a (probably after the H7 cooling event, Prokopenko *et al.*, 2001b) and covered the entire cold and arid stages MIS4 and MIS3. In MIS4, mountain glaciers occurred in the Lake watershed and permafrost covered the other areas (Grachev *et al.*, 1998; Back *et al.*, 1999; Chlachula, 2001). MIS3 was a period with very low lake bioproductivity (Edlund and Stoermer 2000, Prokopenko *et al.*, 2001a, 2001b), and at least the early part of MIS3 was rather cold and dry with loess depositions in river valleys east of Baikal and possibly only episodic warming events (Chlachula *et al.*, 2001).

https://doi.org/10.1346/CCMN.2005.0530407 Published online by Cambridge University Press

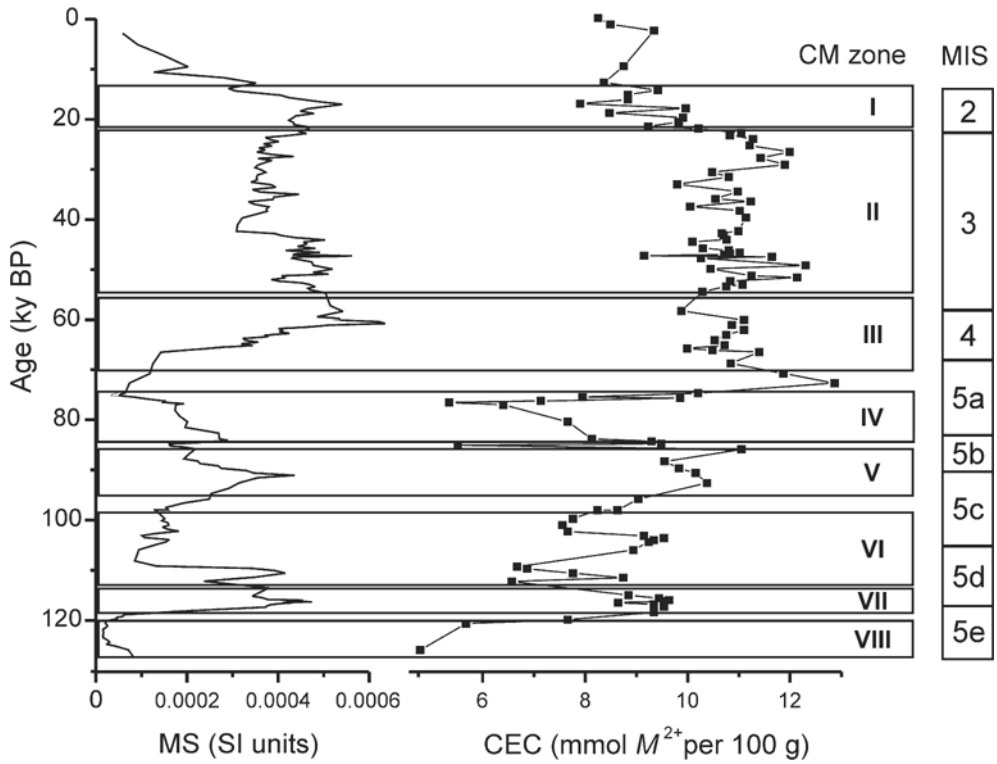

Figure 8. MS and CEC plotted *vs.* the sediment age. Clay mineralogical zones (CM, Table 4) are indicated by rectangles and Roman numerals, marine isotopic stages (MIS) are shown for comparison in the right part of the plot (rectangles with the usual abbreviations).

On the other hand, the most pronounced CEC minima were found at ~120 ky BP, ~100 ky BP and 84–75 ky BP, which correspond to warm parts of the last interglacial: MIS5e, MIS5c and MIS5a, respectively. This pattern of CEC values, corresponding to warm periods with decreased CEC contradicts the assumption of enhanced chemical weathering of primary minerals in warmer periods (Yuretich *et al.*, 1999; Horiuchi *et al.*, 2000; Solotchina *et al.*, 2002). Another rather unexpected result is the increase in the relative content of chlorite in MIS5 with respect to MIS3 (Tables 3 and 4) although the chlorite was expected to be weathered in warmer periods (Fagel *et al.*, 2003).

Under the cold climate of MIS4 and MIS3 (CM zone II) and especially in the last glacial maximum (CM zone I), it is unlikely that the environmental conditions permitted neoformation of substantial amount of smectites or vermiculite. The high CEC values in these periods indicate that there was some pool of expandable clay minerals available in the watershed. That pool could possibly be soils formed under the much warmer climate during the Pliocene (Grachev *et al.*, 1998; Müller *et al.*, 2001), and the transport mechanism especially efficient during the dry and cold climate could be wind. The 'switches' between rivers carrying most sediment in warm periods and wind in cold periods could substantially affect the actual sediment source area. Adversely, the total CEC is most dramatically decreased in the warmer intervals although one could expect the neoformation of smectites from the primary amphiboles, micas and chlorite. If there really was a substantial neoformation of expandable clay minerals in the warmer periods of the late Quaternary, they would either be diluted by the diatom frustules that comprise 0–40% of the Baikal sediments (Peck *et al.*, 1994; Prokopenko *et al.*, 2001a), and/or dissolved in the watershed or in the lake.

It is hence probable that the neoformation of clay minerals in the Lake Baikal watershed was not sufficiently fast to efficiently record the paleoclimatic changes during recent, usually short (5–10 ky) and warm periods: the current mean annual temperature in the Lake Baikal watershed is ~0ºC and annual precipitation is 200–700 mm (Chlachula, 2001), in MIS5e, MIS5c and MIS5a the conditions were probably similar. Such a conclusion is in line with the limits of interpretation of clay mineral ratios in Quaternary marine sediments (Thiry, 2000). In any case, the paleoenvironment has efficiently affected the ECM composition, maybe *via* environmentally driven transport mechanisms, that subsequently produced the easily readable CEC record obtained.

There is a question whether the CEC is only caused by the diatom frustules diluting ECM. However, the varying ratio between chlorite and expandable minerals (Chl/(E2+E3)<0.15 in MIS3 and >0.2 in MIS5) shows that there are some more effects than mere dilution of all components by biogenic SiO_2.

https://doi.org/10.1346/CCMN.2005.0530407 Published online by Cambridge University Press

CONCLUSIONS

The clay mineral assemblage in Academician Ridge sediments of Lake Baikal mirrors the major climatic changes during ~100 ky of the last glacial/interglacial cycle. The amount of expandable clay structures was ascertained from CEC determined by a very convenient and efficient Cu-trien method which has not been used before to analyze sedimentary series. The amount of expandable clay structures followed a pattern of significant content during cold periods and decreased content in warmer periods. Although the mechanism of this environmental imprint is not clear, it operated with the time resolution sufficient for reflecting sub-Milankovitch events such as mid-MIS5c climate deterioration lasting a few ky. This fast response points to a change in the sediment source area rather than to neoformation of clay minerals. The variable ratios between individual clay minerals were visualized by distinguishing the basal diffractions of expandable and non-expandable clay minerals by monitoring their thermal behavior between 25 and 250ºC using HT-XRD.

ACKNOWLEDGMENTS

The authors are grateful to Jerry McManus (Woods Hole Oceanographic Institute, Massachusetts, USA) for kindly providing the reference data for the isotopic composition of the North Atlantic sea water used to construct our age model. The sediment series was provided by GFZ Potsdam, Germany, its sampling and MS measurement were supported by the 5th framework project of the European Commission (CONTINENT project, EVK2-2000-00057), and CM analyses by the Grant Agency of the Czech Republic (IAA3032401). The authors thank Dr Z. Weiss (Technical University Ostrava, Czech Republic) for providing a reference sample of vermiculite.

REFERENCES

Antipin, V., Afonina, T., Badalov, O., Bezrukova, E., Bukharov, A., Bychinsky, V., Dmitriev A.A., Dorofeeva, R., Duchkov, A., Esipko, O., Fileva, T., Gelety, V., Golubev, V., Goreglyad, A., Gorokhov, I., Gvozdkov, A., Hase, Y., Ioshida, N., Ivanov, E., Kalashnikova, I., Kalmychkov, G., Karabanov, E., Kashik, S., Kawai, T., Kerber, E., Khakhaev, B., Khlystov, O., Khursevich, G., Khuzin, M., King, J., Konstantinov, K., Kochukov, V., Krainov, M., Kravchinsky, V., Kudryashov, N., Kukhar, L., Kuzmin, M., Nakamura, K., Nomura, S., Oksenoid, E., Peck, J., Pevzner, L., Prokopenko, A., Romashov, V., Sakai, H., Sandimirov, I., Sapozhnikov, A., Seminsky, K., Soshina, N., Tanaka, A., Tkachenko, L., Ushakovskaya, M. and Williams, D. (2001). The new BDP-98 600-m drill core from Lake Baikal: a key late Cenozoic sedimentary section in continental Asia. *Quaternary International*, **80-81**, 19–36.

Back, S., De Batist, M., Strecker, M.R. and Vanhauwaert, P. (1999) Quaternary depositional systems in Northern Lake Baikal, Siberia. *Journal of Geology*, **107**, 1–12.

Bérend, I., Cases, J.M., Bérend, I., François, M., Uriot, J.P., Michot, L., Maison, A. and Thomas, F. (1995) Mechanism of adsorption and desorption of water vapor by homoionic montmorillonite: 3. Li^+, Na^+, Rb^+, and Cs^+ exchanged forms. *Clays and Clay Minerals*, **43**, 324–336.

Bray, H., Redfern, S.A.T. and Clark, S.M. (1998) The kinetics of dehydration in Ca-montmorillonite: an *in situ* X-ray diffraction study. *Mineralogical Magazine*, **62**, 647–656.

Cases, J.M., Bérend, I., François, M., Uriot, J.P., Michot, L.J. and Thomas, F. (1997) Mechanism of adsorption and desorption of water vapor by homoionic montmorillonite: 3. Mg^{2+}, Ca^{2+}, Sr^{2+}, and Ba^{2+} exchanged forms. *Clays and Clay Minerals*, **45**, 8–22.

Chlachula, J. (2001) Pleistocene climate change, natural environment and Paleolithic occupation of the Angara-Baikal area, east Central Siberia. *Quaternary International*, **80-81**, 69–62.

Collins, D.R., Fitch, A.N. and Catlow, C.R.A. (1992) Dehydration of vermiculites and montmorillonites: A time resolved powder neutron diffraction study. *Journal of Materials Chemistry*, **2**, 865–873.

Demory, F., Oberhansli, H., Nowaczyk, N.R., Gottschalk, M., Wirth, R. and Neumann, R. (2005) Detrital input and early diagenesis in sediments from Lake Baikal revealed by rock magnetism. *Global and Planetary Change*, **46**, 145–166.

Edlund, M.B. and Stoermer, E.F. (2000) A 200,000-year, high-resolution record of diatom productivity and community makeup from Lake Baikal shows high correspondence to the marine oxygen-isotope record of climate change. *Limnology and Oceanography*, **45**, 948–962.

Fagel, N., Boski, T., Likhoshway, L. and Oberhansli, H. (2003) Late Quaternary clay mineral record in Central Siberia Lake Baikal (Academician Ridge, Siberia). *Palaeogeography Palaeoclimatology Palaeoecology*, **193**, 159–179.

Grachev, M.A., Vorobyova, S.S., Likhoshway, Y.V., Goldberg, E.L., Zbirova, G.A., Levina, O.V. and Khlystov, O.M. (1998) A high-resolution diatom record of the palaeoclimates of East Siberia for the last 2.5 My from Lake Baikal. *Quaternary Science Reviews*, **17**, 1101–1106.

Graf von Reichenbach, H. and Beyer, J. (1994) Dehydration and rehydration of vermiculites: I. Phlogopitic Mg-vermiculite. *Clay Minerals*, **29**, 327–340.

Horiuchi, K., Minoura, K., Hoshino, K., Oda, T., Nakamura, T. and Kawai, T. (2000) Palaeoenvironmental history of Lake Baikal during the last 23000 years. *Palaeogeography Palaeoclimatology Palaeoecology*, **157**, 95–108.

Kaufhold, S., Dohrmann, R., Ufer, K. and Meyer, F.M. (2002) Comparison of methods for the quantification of montmorillonite in bentonites. *Applied Clay Science*, **22**, 145–151.

Kravchinsky, V.A., Krainov, M.A., Evans, M.E., Peck, J.A., King, J.W., Kuzmin, M.I., Sakai, H., Kawai, T. and Williams, D.F. (2003) Magnetic record of Lake Baikal sediments: chronological and paleoclimatic implication for the last 6.7 Myr. *Palaeogeography Palaeoclimatology Palaeoecology*, **195**, 281–298.

Laureiro, Y., Jerez, A., Rouquérol, F. and Rouquérol, J. (1996) Dehydration kinetics of Wyoming montmorillonite studied by controlled transformation rate thermal analysis. *Thermochimica Acta*, **278**, 165–173.

Marcos, C., Arguelles, A., Ruiz-Conde, A., Sanchez-Soto, P.J. and Blanco, J.A. (2003) Study of dehydration process of vermiculites by applying a vacuum pressure: formation of interstratified phases. *Mineralogical Magazine*, **67**, 1253–1268.

McManus, J.F., Oppo, D.W. and Cullen, J.L. (1999) A 0.5-million-year record of millennial-scale climatic variability in the North Atlantic. *Science*, **283**, 971–975.

McManus, J.F., Oppo, D.W., Keigwin, L.D., Cullen, J.L. and Bond, G.C. (2002) Thermohaline circulation and prolonged interglacial warmth in the North Atlantic. *Quaternary Research*, **58**, 17–21.

Meier, L.P. and Kahr, G. (1999) Determination of the cation

exchange capacity (CEC) of clay minerals using the complexes of copper(II) ion with triethylenetetramine and tetraethylenepentamine. *Clays and Clay Minerals*, **47**, 386–388.

Moore, D.M. and Hower, J. (1986) Ordered interstratification of dehydrated and hydrated Na-smectite. *Clays and Clay Minerals*, **34**, 379–384.

Müller, J., Oberhansli, H., Melles, M., Schwab, M., Rachdol, V. and Hubberten, H.-W. (2001) Late Pliocene sedimentation in Lake Baikal: implications for climate and tectonic change in SE Siberia. *Palaeogeography Palaeoclimatology Palaeoecology*, **174**, 305–326.

Peck, J.A., King, J.W., Colman, S.M. and Kravchinsky, V.A. (1994) A rock-magnetic record from Lake Baikal, Siberia: Evidence for Late Quaternary climatic change. *Earth and Planetary Science Letters*, **122**, 221–238.

Prokopenko, A.A., Karabanov, E.B., Williams, D.F., Kuzmin, M.I., Shackleton, N.J., Crowhurst, S.J., Peck, J.A., Gvozdkov, A.N. and King, J.W. (2001a) Biogenic silica record of Lake Baikal response to climatic forcing during the Brunhes. *Quaternary Research*, **55**, 123–132.

Prokopenko, A.A., Karabanov, E.B., Williams, D.F., Kuzmin, M.I., Khursevich, G.K. and Gvozdkov, A.N. (2001b) The detailed record of climatic events during the past 75,000 yrs BP from the Lake Baikal drill core BDP-93-2. *Quaternary International*, **80-81**, 59–68.

Ruiz-Conde, A., Ruiz-Amil, A., Perez-Rodriguez, J.L. and Sanchez-Soto, P.J. (1996) Dehydration-rehydration in magnesium vermiculite: conversion from two-one and one-two layer hydration states through the formation of interstratified phases. *Journal of Materials Chemistry*, **6**, 1557–1566.

Singer, A. (1979/1980) The paleoclimatic interpretation of clay minerals in soils and weathering profiles. *Earth Science Reviews*, **15**, 303–326.

Solotchina, E.P., Prokopenko, A.A., Vasilevsky, A.N., Gavshin, V.M., Kuzmin, M.I. and Williams, D.F. (2002) Simulation of XRD patterns as an optimal technique for studying glacial and interglacial clay mineral associations in bottom sediments of Lake Baikal. *Clay Minerals*, **37**, 105–119.

Thiry, M. (2000) Palaeoclimatic interpretation of clay minerals in marine deposits: an outlook from the continental origin. *Earth Science Reviews*, **49**, 201–221.

Weiss, Z., Valvoda, V. and Chmielová, M. (1994) Dehydration and rehydration of natural Mg-vermiculite. *Geologica Carpathica Series Clays*, **45**, 33–39.

Yuretich, R., Melles, M., Sarata, B. and Grobe, H. (1999) Clay minerals in the sediments of Lake Baikal: A useful climate proxy. *Journal of Sedimentary Research*, **69**, 588–596.

(*Received 5 December 2004; revised 2 March 2005; Ms. 987; A.E. Warren D. Huff*)